INTEGRATION OF FIBER BRAGG GRATINGS IN WOVEN FABRICS: INFLUENCES OF PREFORM COMPACTION AND FLOW-FRONT PROPAGATION

J. M. Balvers[1], H. E. N. Bersee[1], and A. Beukers[1]

[1]*Faculty of Aerospace Engineering, Delft University of Technology,*
Kluyverweg 1, 2629 HS Delft, The Netherlands
Corresponding author's Email: J.M.Balvers@TUDelft.nl

SUMMARY: In order to reduce structural defects and improve quality and reliability of Advanced Composites (ACs), it is generally recognized that the manufacturing process of ACs should be monitored *in situ* and on-line. Up to now, the most adequate or promising technique for *in situ* and on-line cure monitoring during manufacturing of ACs in combination with in-service structural integrity evaluation seems to be based on optical techniques. In this paper, the role of optical fibers with multiple Fiber Bragg Gratings (FBG) is investigated in composites processing. In an experimental vacuum infusion set-up, the effects of fabric compaction and flow-front propagation on the measured strain were studied. It can be concluded that both the fabric compaction and flow-front propagation can be monitored. However, no quantitative description is obtained. Due to global effects such as small-radius bending, additional strain distributions are observed that influence negatively the reading of the point sensors. It is, therefore, questionable whether to take into account these processing steps in strain calculations.

KEYWORDS: Fiber Bragg Gratings (FBG), flow monitoring, compaction of preform, vacuum infusion

INTRODUCTION

In order to reduce structural defects and to improve quality and reliability of Advanced Composites (ACs), it is generally recognized that the manufacturing process of ACs should be monitored *in situ* and on-line. With monitoring, the classical manufacturing process will change to smart processing, in which sensors perform real-time identification of material properties [1]. Furthermore, *in situ* monitoring as a non-destructive inspection method will probably shorten the time needed for qualification of new AC structures, improve the quality of manufacturing, and decrease the rejection rate of parts failed to match the predefined criteria [2]. Up to now, the most adequate or promising technique for *in situ* and on-line cure monitoring during manufacturing of ACs in combination with in-service structural integrity evaluation seems to be based on optical techniques [3-5]. With optical fiber sensors, engineers get the opportunity to add a nervous system to their designs which enables several capabilities to AC structures [6].

For temperature, strain, or other parameters that need to be quantified by measurement in ACs, several optical fiber-based sensor techniques have been developed in the recent years. One of these techniques is based on fiber Bragg gratings (FBG). Briefly explained, a Bragg grating in an optical fiber, which is illuminated by a broadband spectrum light, reflects a narrow-band optical signal, satisfying the Bragg condition, at a particular wavelength (i.e., the Bragg wavelength, λ_B), whereas all other wavelengths of the broadband spectrum light are transmitted. Temperature and strain changes are simultaneously and indirectly measured by the change in the Bragg wavelength.

As a part of a major project, several aspects have been investigated that are related to the integration of these FBGs in the manufacturing process of thick-walled ACs. Although, eventually, the thick-walled ACs will be produced with the Resin Transfer Molding (RTM) process, the experiments in this paper are carried out using the Vacuum Infusion (VI) process. Both the RTM process and VI process belong to the group of Liquid Composite Molding (LCM) techniques, which are characterized by four different stages: preforming, injection, curing, and demolding of the final product. Since residual stresses could have detrimental effects on the quality of ACs, monitoring the curing step is of up most importance. With FBGs not only local information about the reaction temperature could be obtained but one could also measure the strain development during the reaction. However, is the measured strain in the curing stage identical to the overall process strain or do the preceding steps (i.e., preforming and injection) also contribute to the total strain? In other words, what is the effect of the preceding steps on the signal output of the sensor? Do we have to take these steps into account or is it satisfactory to look only at the curing stage when strains have to be determined? What will be the reference level: before the process starts, in between the injection and curing stages, or somewhere else? To answer these questions this paper goes into more detail on how the FBG is influenced by the compaction pressure (i.e., the preforming stage) and flow-front propagation (i.e., the injection stage) for woven fabrics. Based on the observations, conclusions will be drawn with respect to the importance of these stages on strain development.

THEORETICAL BACKGROUND

As explained in the introduction, FBGs reflect a narrow-band optical signal when the optical fiber is illuminated by a broadband spectrum. The reflection is caused by a periodic modulation of the refractive index of a segment of the core (Fig. 1).
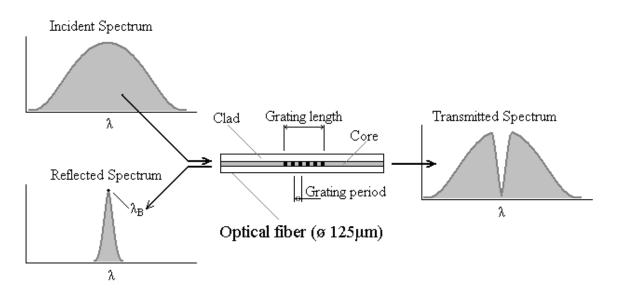
Fig. 1 The fiber Bragg grating structure.

The wavelength, at which this narrow-band optical signal is reflected, is called the Bragg wavelength and is defined as follows:

$$\lambda_B = 2\, n_{eff}\, \Lambda \tag{1}$$

where n is the effective refractive index of the grating and Λ is the grating period [7,8]. According to this expression, a shift in the Bragg wavelength will be observed when either the effective refractive index or the grating period is changed. Thus, strain and thermal effects that will modify the physical or geometric properties of the grating can be monitored through looking at the shift in the Bragg wavelength. In this paper, the following expression is used to calculate the Bragg wavelength shift due to mechanical (strain: ε) and thermal loading (temperature: T):

$$\Delta\lambda_B\, /\, \lambda_B = (1 - P)\, \Delta\varepsilon + (\alpha_n + \alpha_f)\, \Delta T = S_\varepsilon\, \Delta\varepsilon + S_T\, \Delta T \tag{2}$$

in which P is the effective photo-elastic coefficient or strain-optic coefficient, α_n is the thermo-optic constant, and α_f is the thermal expansion coefficient of the optical fiber. The factors S_ε and S_T represent the strain and temperature sensitivities, respectively. Although the derivation of this expression is not complicated, it is beyond the scope of this paper to go into more detail. A clear description of this derivation can be found in Ref. 8.

In addition, it is assumed that the thermal effects can be neglected. All experiments, which will be explained in the next section, are performed at room temperature. During these experiments care has been taken to minimize temperature fluctuations. Consequently, the right term on the right-hand side can be omitted because ΔT equals zero. After rearranging Eqn. 2, the equation becomes:

$$\Delta\varepsilon = (1\, /\, S_\varepsilon)\, \Delta\lambda_B\, /\, \lambda_B \tag{3}$$

This relationship, between the shift in the Bragg wave length and the change in strain, will be used to characterize the influence of compaction and flow-front propagation on the signal. The optical fibers used in the experiments have a strain sensitivity of 0.78.

EXPERIMENTAL PROCEDURES

From a chronological point of view, preform compaction is the first step after the initial preparations such as fabric cutting, shaping of preform, placement of preform in the mold cavity, placement of inlets/vents and finally vacuum bagging.

In order to study the influence of preform compaction, the VI process of a rectangular flat-plate thin-walled AC is imitated. That is, four layers of woven fabric (*i*) are placed on top of a stiff metal plate (*ii*). Between the second and third layer an optical fiber (*iii*) with multiple FBGs (1-3) is embedded, which is connected to an interrogator (*iv*) and a PC (*v*) for monitoring the wavelength shift. A vent (transparent tube) (*vi*) is on one side fixed near the preform and the other side is connected to a resin trap (*vii*) and a vacuum pump (*viii*), which has a portable barometer (GDH 200 of GREISINGER Electronic) (*ix*) to indicate the absolute pressure inside the vacuum bagged system. Finally, the mold is covered with a vacuum bag. The experimental set-up is schematically shown in Fig. 2.
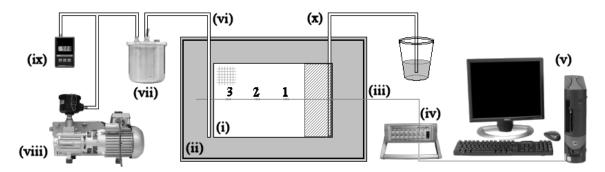

Fig. 2 Experimental test set-up.

The second step is the injection itself. A similar experimental set-up has been used to monitor flow behavior. In case of these flow-front propagation experiments, an additional transparent tube (*x*), which acts as an inlet, is added to the system (Fig. 2).

For the first group of experiments, the procedure is to first apply vacuum and let the preform be compacted. After stabilization of the signal, the vacuum is then released to ambient pressure. This step is repeated for different pressure levels (in the range of absolute vacuum to ambient pressure). In this way, the wavelength shift (and thus strain) could be related to the compaction pressure, which is obtained from the barometer.

In case of the second group, a test fluid replaces the reactive resin system in order to reuse the optical fiber. The test fluid is an aqueous glycerin solution with a weight ratio of 90:10 (10 parts of water). With this ratio, the viscosity becomes comparable to the one of a reactive resin system. After mixing the aqueous glycerin solution and applying vacuum, the fluid is injected via the

inlet. As soon as the fluid reaches the vent, the vacuum pump is turned off and the measurement is stopped.

In both experiments several factors were identified that could influence the output signal. Not only the type of fabric but also the orientation of the optical fiber with respect to the fabric could play an important role. However, the results of these experiments are not yet taken into account in this paper.

RESULTS AND DISCUSSION

Initial Experiments

As a starting point, two experiments (one of each group) were performed. In Fig. 3 the results of these experiments are presented. On the left-hand side one sees the results of the fabric compaction test and on the right-hand side the results are shown of monitoring the injection. Both experiments were performed using a single optical fiber with three 4mm FBGs with a mutual distance of 70mm. The optical fiber was embedded between fine woven fabrics (7HS weave pattern). Care was taken to align the optical fiber with the warp direction, which is defined as 0º orientation. All three FBGs were placed in a straight line and the optical fiber was attached to the mold in such a way that it could move freely in longitudinal direction. Fig. 2 shows schematically the test set-up.
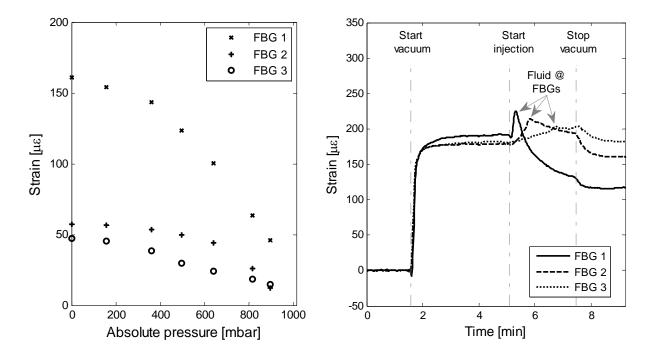
Fig. 3 Initial tests: effect of fabric compaction (left) and flow-front propagation (right).

From the results the following initial conclusions were drawn. Compaction of the fabric by applying vacuum results in straining the optical fiber. The more the absolute pressure is reduced

the larger becomes the strain. Although this behavior is observed by all three FBGs, FBG 1 measures a strain that is three to four times larger than the ones observed by the other FBGs. Initially, this difference was related to the placement of the optical fiber with respect to the fabric. As will be explained later on in this section, it turned out that other effects are probably more dominating.

Looking at the graph at the right-hand side of Fig. 3, the following conclusions were drawn with respect to monitoring flow-front propagation. Applying vacuum (absolute pressure of 40-50 mbar) resulted in straining of the optical fiber. All three FBGs reacted similar. They stabilized within two minutes and reached more or less the same strain level (i.e., 170-180 με). Compared to the previous experiment, the mutual difference between the FBGs is smaller. As soon as the liquid started to impregnate the fabric the signals of the FBGs started to deviate. The FBG closest to the inlet (i.e., FBG 1) showed the steepest increase, whereas FBG 3, which is farthest from the inlet, had the lowest strain rate. It cannot be caused by an instantaneous temperature change at the FBG location, but is probably caused by a global effect, i.e., an effect that takes place somewhere else then at the location of the FBG (see last section). At the peak values the resin is physically in contact with the FBGs. Directly after the flow-front passed the FBGs the strain started to decrease again. When the resin reached the vent, the vacuum pump was turned off and, as a consequence, another drop in strain is observed.

Parametric Analysis

In several experiments different configurations were tested in order to determine the impact on the signal output. In Table 1 these factors are listed together with their levels.

Table 1 Identified factors for parametric analysis

Factor	Range/Level	
Grating length:	4mm	8mm
Fabric:	fine 7HS	coarse PW
	(tow width of 1mm)	(tow width of 5mm)
Orientation:	0º to 90º	
Clamping:	free to move	fixed
	in longitudinal direction	

The optical fiber with FBGs of grating length 8 mm has also three FBGs at a mutual distance of 70mm. In all experiments these two optical fibers were simultaneously embedded. They were both placed in a straight line and fixed to the mold using one of the two clamping options. The orientation was limited to three levels: 0º, 45º, and 90º with respect to the weft direction of the fabric or flow direction.

Subsequently, it was tried to establish a set of rules that describe the behavior of the optical fiber with respect to these configurations. However, a large spread in measured data was observed in both groups of experiments making it difficult to quantitatively describe the influence of these factors. In general, similar trends were observed in all experiments: applying vacuum results in a change in strain level and the FBG reacts on flow-front propagation. But no consistency was

observed. Not only were the strain levels after compaction different for each individual FBG but also the stabilization periods seemed to be randomly. Furthermore, repeating similar injection experiments never resulted in similar output. The FBGs react on fluid propagation, but never in the same fashion. So, what causes these deviations?

Global Effects that Affect the Response

Compared to the scale of the laminates, in which the optical fibers are embedded, FBGs (with a grating length of several millimeters) should be considered as being point sensors. It means, any information that is obtained from the sensor should be related to the location of the FBG. However, is the measured strain really coming from this location? In fact, one is often dealing with multiple FBGs in a single optical fiber. Each FBG (read: measurement point) is connected to other FBGs via the optical fiber. When the fabric is compacted, not only the parts of the optical fiber containing the gratings are affected but also the optical fiber in between. Although the connecting parts do not act as sensors, they may still cause an additional strain distribution in the optical fiber and, thus, disturb the reading.

One of the main contributions to these disturbances comes from small-radius bending of the optical fiber due to either compaction of the fabric or fluid flow. In Fig. 4 this is schematically represented. In this example, which has been verified with experiments, the FBG is placed inside a steel capillary. As one can see, compaction causes bending of the optical fiber at the ends of the capillary. These bending points act as clamping points and the optical fiber must elongate on either side. Consequently, an increase in strain is measured by the FBG due to this bending. This is in contradiction of what would be expected: the FBG should not measure any change in strain due to fabric compaction, because it is encapsulated in a stiff capillary. Small-radius bending of the optical fiber not only happens in combination with a capillary, but also at the edges where the optical fiber comes out of the preform. Furthermore, the flow-front may also cause bending, because the compaction pressure field ahead of the flow-front is different compared to the one behind the flow-front due to the presence of a fluid pressure field. The fluid causes expansion of the preform and, consequently, bending of the optical fiber.

Another disturbing factor may be caused by the vacuum bag itself. When vacuum is applied, the air is removed. Most times folds are automatically created because of excessive bagging material. These folds are randomly distributed and seem to influence the measured strain.
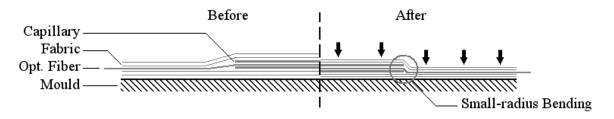

Fig. 4 Bending of the optical fiber by fabric compaction: before and after compaction.

CONCLUSIONS

Based on the observations from the experimental work it can be concluded that one should take care when reading out the data from embedded optical fibers in woven fabrics. During preform compaction and fluid injection strains are measured that not only come from the local measuring point (i.e., location of the FBG). Small-radius bending of another part of the optical fiber could easily result in an additional strain distribution, which disturbs the local strain profile observed at the FBG location. Several causes of small-radius bending have been mentioned and all of them negatively affect the reading. Unless the FBGs are protected from these events, the measured response may become useful. Otherwise, it would be wise not to attach too much importance to the change in strain caused in the fabric compaction and injection steps of the VI process. In the near future, additional experiments will be performed, in which it will be tried to reduce the influence of global effects. Furthermore, the investigation will be enlarged by taking also the curing stage into account.

REFERENCES

1. A. Cusano, G. Breglio, M. Giordano, A. Calabrò, L. Nicolais, "Optoelectronic Characterization of the Curing Process of Thermoset-Based Composites," *Journal of Optics A: Pure and Applied Optics*, Vol. 3, No. 2, 2001, pp. 126-130.

2. P. Ferdinand, S. Magne, V. Dewynter-Marty, S. Rougeault, L. Maurin, "Applications of Fiber Bragg Grating Sensors in the Composite Industry," *MRS Materials Research Society Bulletin* [online journal], May 2002, URL: http://www.mrs.org

3. V. Antonucci, M. Giordano, A. Cusano, J. Nasser, L. Nicolais, "Real Time Monitoring of Cure and Gelification of a Thermoset Matrix," *Composites Science and Technology*, Vol. 66, No. 16, 2006, pp. 3273-3280.

4. E. Chailleux, M. Salvia, N. Jaffrezic-Renault, V. Matejec, I. Kasik, "In-Situ Study of the Epoxy Cure Process using a Fiber-Optic Sensor," *Smart Materials and Structures*, Vol. 10, No. 2, 2001, pp. 194-202.

5. J. Leng, A. Asundi, "Structural Health Monitoring of Smart Composite Materials by using EFPI and FBG Sensors," *Sensors and Actuators A*, Vol. 103, No. 3, 2003, pp. 330-340.

6. T.S. Jang, J.J. Lee, D.C. Lee, J.-S. Huh, "The Mechanical Behavior of Optical Fiber Sensor embedded within the Composite Laminate," *Journal of Materials Science*, Vol. 34, No. 23, 1999, pp. 5853-5860.

7. K.S.C. Kuang, L. Zhang, W.J. Cantwell, I. Bennion, "Process Monitoring of Aluminum-Foam Sandwich Structures based on Thermoplastic Fiber-Metal Laminates using Fiber Bragg Gratings," *Composites Science and Technology*, Vol. 65, No. 3-4, 2005, pp. 669-676.

8. M. Giordano, A. Laudati, J. Nasser, L. Nicolais, A. Cusano, A. Cutolo, "Monitoring by a single fiber Bragg grating of the process induced chemo-physical transformations of a model thermoset," *Sensors and Actuators A*, Vol. 113, No. 2, 2004, pp. 166-173.